Journal of Applied Polymer Science

Preparation and Properties of a Polyether-Based Polycarboxylate as an Antiscalant for Gypsum

Ke Cao,[1] Yuming Zhou,[1] Guangqing Liu,[1] Huchuan Wang,[1] Wei Sun[2]

[1]School of Chemistry and Chemical Engineering, Southeast University, Nanjing 211189, Jiangsu, People's Republic of China

[2]Product Department, Jianghai Environmental Protection Co., Ltd, Zhenglu Zhen, Changzhou 213116, Jiangsu, People's Republic of China

Correspondence to: Y. Zhou (E-mail: ymzhou@seu.edu.cn)

ABSTRACT: A polyether-based copolymer of acrylic acid-allylpolyethoxy maleic carboxylate (AA-APEY) was prepared by copolymerization of allylpolyethoxy carboxylate (APEY) and acrylic acid (AA) at different mole ratios. The main aim of this work was to investigate the influence of AA-to-APEY mole ratios on the copolymer properties and scale inhibition performance for gypsum. The synthesized copolymer was characterized by Fourier-transform infrared (FT-IR) and further conformed by ^{1}H NMR. The effect of AA-APEY on controlling calcium sulfate deposits was studied through static scale inhibition tests under standard solution conditions. And the result was compared with that of other polycarboxylates, which are similar to AA-APEY in structure. Scanning electronic microscopy (SEM), transmission electron microscopy (TEM), and X-ray powder diffraction (XRD) analysis were carried out to study the morphology and structure changes of calcium sulfate crystals in the presence of AA-APEY. © 2013 Wiley Periodicals, Inc. J. Appl. Polym. Sci. **2014**, *131*, 40193.

KEYWORDS: copolymers; thermal properties; properties and characterization

Received 24 September 2013; accepted 15 November 2013

DOI: 10.1002/app.40193

INTRODUCTION

In recent years, polycarboxylate is one of the polymers most widely applied as an antiscalant. As known, the formation of mineral precipitation in many chemical equipments, such as heat exchangers and water pipes, has historically been a problem for industrial recycling cooling system.[1,2] Scale deposits may cause efficiency losses in heat transmission and thus increase the water usage and industrial costs. Common calcium depositions, for example, calcium carbonate ($CaCO_3$) and calcium sulfate ($CaSO_4$, commercially known as gypsum), are easy to precipitate because of their inverse temperature solubility characteristics.[2] However, $CaSO_4$ is more difficult to remove as the spontaneous precipitate process of gypsum is not concentration dependent.[3,4] A common method to control $CaSO_4$ precipitation is by addition of antiscalants, which are water-soluble salts or polymers containing functional groups. The most effective groups include phosphonate, carboxylate, and sulfonate.[5,6]

Conventionally, inhibitors are classified as inorganic salts and organic polymer compounds. Inorganic scale inhibitors, such as sodium hexametaphosphate[7] and sodium pyrophosphate,[8] were explored and widely used in the initial period of chemical water treatment industry. Polyphosphates[9–12] and polycarboxylates,[13,14] which have a remarkable ability to chelate calcium-ions, are major organic inhibitors in current recycling water systems.[15] However, both inorganic phosphates and organic phosphorus products are unstable in water because that they would hydrolyze to ineffective orthophosphate and then form calcium phosphate deposits in the presence of certain calcium-ions.[16–19] In addition, phosphorus pollution is considered the key factor of eutrophication, which is by far the most serious problem on water pollution.[20] Recently, a new kind of polyether-based polymer was reported as polycarboxylate antiscalant for $CaSO_4$ deposition. There were allylpolyethoxy carboxylate (APEC) reported by Du[21] and ammonium allylpolyethoxy sulfate (APES) reported by Steckler.[22] Both APEC and APES have carboxylic acid (—COOH) groups, which can make it functional material to control mineral scale for different recycling cooling water qualities. APES products have been widely applied in water treatment industry currently. Amjad[14] showed that copolymer scale inhibitors containing —COOH groups such as poly(acrylic acid) and poly(maleic acid) were particularly effective to retard $CaSO_4$ deposition. Nevertheless, chloracetic acid and sulfamic acid, which are used in the synthesis of APEC and APES, are unfriendly to water environment.

In view of the above, many polymeric antiscalants have been widely used to retard the crystallization of calcium sulfate, but the efficiency is low on both economic and environmental

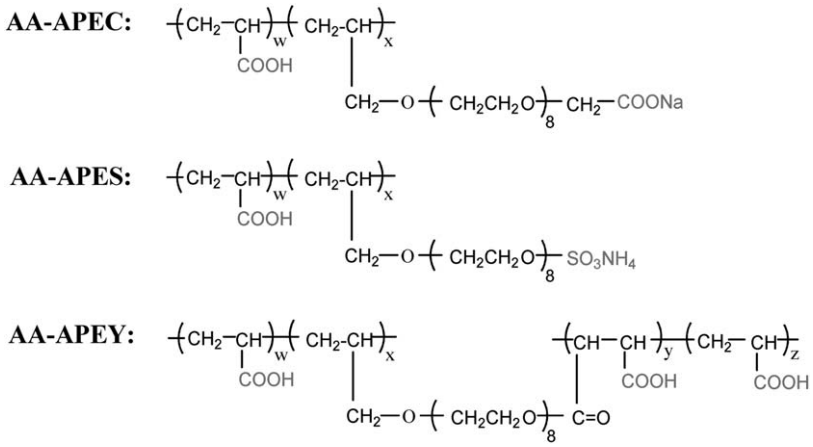

Scheme 1. The structures of AA-APEC, AA-APES, and AA-APEY.

grounds. Therefore, the synthesis and application of green inhibitors are the focus of further research and form the crux of this article. The aim of this article is to provide a "green" copolymer of acrylic acid-allylpolyethoxy maleic carboxylate (AA-APEY or AY) as an ideal $CaSO_4$ scale inhibitor. To improve the degree of carboxylation, maleic anhydride (MA) was used in the synthesis of APEY. The designed double-hydrophilic block copolymers, linking with more carboxylate-terminated side chains, were prepared through free radical solution copolymerization. After analyzing the characterization studies, AY was evaluated as a potential antiscalant for preventing $CaSO_4$ scale-deposits using simulated water solutions.

EXPERIMENTAL

Materials

Acrylic acid (AA), maleic anhydride (MA) and ammonium persulfate (APS) were analytically pure grade and was supplied by Zhongdong Chemical Reagent (Nanjing, Jiangsu, People's Republic of China). Allyloxy poly(ethylene glycol) (APEG, $M_W = 400$ g mol^{-1}), acrylic acid-allylpolyethoxy carboxylate (AA-APEC, $M_W = 15{,}000$ g mol^{-1}) and acrylic acid-ammonium allylpolyethoxy sulfate (AA-APES, $M_W = 20{,}000$ g mol^{-1}) were supplied by Jiangsu Jianghai Chemical (Changzhou, Jiangsu, People's Republic of China). APEY was synthesized from APEG, which has the same amount of repeating units (ethylene oxide, $n = 8$) with APEC and APES. The structures of AA-APEC, AA-APES and AA-APEY are depicted in Scheme 1. Distilled water was used in the course of entire experiment.

Synthesis of APEY

Allylpolyethoxy maleic carboxylate (APEY) was synthesized in our laboratory according to previous studies by Du.[21] APEG was carboxylate-terminated using MA with a molar ratio of 1 : 1 in high yields exceeding 98.9%.The synthesis procedure of APEY is shown in Scheme 2.

Synthesis of AA-APEYs

A typical synthetic process is as follows: a four-neck round bottom flask, equipped with a magnetic stirrer and a thermometer, was filled with 25.0 g APEY and 60 mL distilled water and heated to 70°C with stirring under nitrogen atmosphere. After that, various amounts of AA in 18 mL distilled water and the initiator solution (3.0 g APS in 17 mL distilled water) were added through different necks in 1.0 h. The dosage of AA was calculated previously to insure the AA/APEY mole ratios (5 : 1, 3 : 1, 1 : 1, 1 : 3, 1 : 5). After that, the flask was heated to 80°C with stirring until the color of solution changed. Finally, the purified products, containing ~25% solid, were used for inhibition tests. The synthesis procedure of AA-APEY is given in Scheme 3.

Static Scale Inhibition Methods

All precipitation experiments were carried out with simulated solutions according to earlier publications[23] and all inhibitor dosages given below are on a dry-inhibitor basis. Calcium sulfate precipitation and inhibition were studied in artificial cooling water which was prepared by dissolving a certain quantity of $CaCl_2$ and Na_2SO_4 in deionized water according to the national standard of P. R. China concerning the code for the design of industrial recirculating cooling-water treatment (SY/T 5673-93). The prepared solutions, 250 mL of $CaC1_2$ (13,600 mg L^{-1} Ca^{2+}) and 250 mL of Na_2SO_4 (14,200 mg L^{-1} SO_4^{2-}), were kept in separate glass bottles at room temperature for 5 h to stabilize their temperature. After that, these solutions were mixed in a suitable flask which had been placed in a thermostatic water bath. The artificial cooling water containing different dosages of antiscalants was thermostated at 70°C for 6 h.

All Ca^{2+} ions concentration was then standardized through ethylenediaminetetraacetic acid (EDTA) titrimetric method. Inhibition efficiency as a calcium sulfate inhibitor was calculated from the following equation:

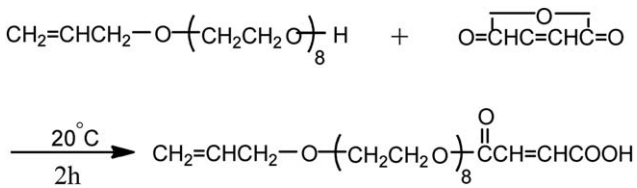

Scheme 2. Synthesis procedure of APEY.

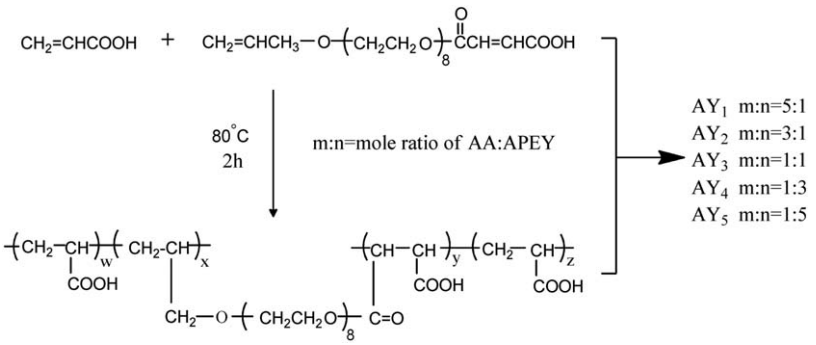

Scheme 3. Synthesis procedure of AA-APEY.

$$\eta(\%) = \frac{[Ca^{2+}]_{final} - [Ca^{2+}]_{blank}}{[Ca^{2+}]_{initial} - [Ca^{2+}]_{blank}} \times 100\%$$

where $[Ca^{2+}]_{final}$ and $[Ca^{2+}]_{blank}$ is residual concentration of Ca^{2+} ions after heating at 70°C for 6 h in the presence and absence of inhibitors respectively; $[Ca^{2+}]_{initial}$ is concentration of Ca^{2+} ions at the beginning of the experiment.

Characterization Studies

Molecular weight determinations were performed by gel permeation chromatography (GPC, Shodex KF-850 column) calibrated using polyethylene glycol (PEG) standards ranging in molecular mass from 1.32×10^2 to 1.34×10^6 g mol^{-1}. Water was used as mobile phase at a flow rate of 1.00 mL min^{-1}. Fourier-transform infrared (FT-IR) spectra were tested on a Bruker FT-IR analyzer (VECTOR-22, Bruker, Germany) by using the KBr-pellet method (compressed powder). ^{1}H NMR spectra were recorded on a Mercury VX-500 spectrometer (Bruker AMX500) using tetramethylsilane (TMS) internal reference and deuterated dimethyl sulfoxide (DMSO-d_6) as a solvent. Thermal analysis experiments were performed using a thermal gravimetric analysis apparatus (TGA, TA Q-600, T.A. Instruments) at a heating rate of 10 K min^{-1} in a nitrogen atmosphere with a sample size of ~50 mg. The X-ray diffraction (XRD) patterns of $CaSO_4$ crystals were recorded on a Rigaku D/max 2400 X-ray powder diffractometer with Cu Kα radiation ($\lambda = 1.5406$, 40 kV, 120 mA). The changes of $CaSO_4$ crystal morphology were examined through transmission electron microscope (TEM, JEM-2100SX, Japan) and scanning electron microscope (SEM, S-3400N, HITECH, Japan).

Table I. Average Molecular Weights of YAs

Sample	AA/APEY molar ratio	$M_w \times 10^{-4a}$	$M_n \times 10^{-4a}$	PD
AY_1	5 : 1	1.83	1.75	1.05
AY_2	3 : 1	1.84	1.79	1.03
AY_3	1 : 1	1.96	1.84	1.07
AY_4	1 : 3	1.98	1.84	1.07
AY_5	1 : 5	2.17	1.98	1.10

[a] Determined by GPC eluted with water based on PEG standards.

RESULTS AND DISCUSSION

GPC Analysis of AYs

As shown in Scheme 3, copolymers were prepared through free radical solution copolymerization at different AA/APEY mole ratio. These crude products obtained directly from the bulk

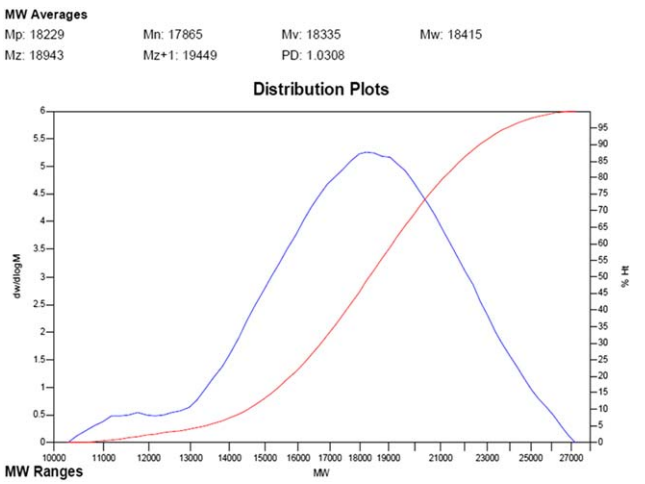

Figure 1. Retention curve profiles of AY_2. [Color figure can be viewed in the online issue, which is available at wileyonlinelibrary.com.]

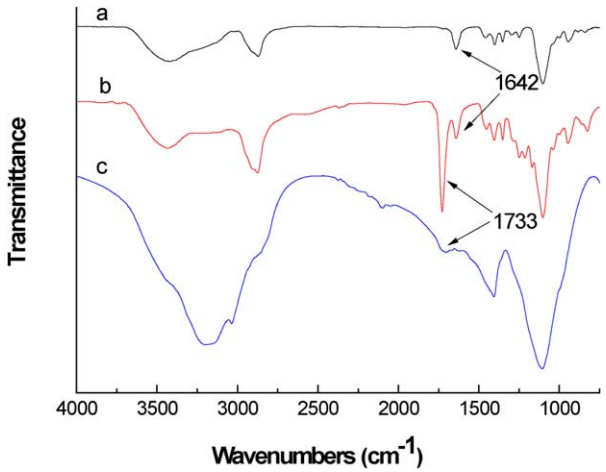

Figure 2. FT-IR spectra of APEG (a), APEY (b), and AA-APEY (c). [Color figure can be viewed in the online issue, which is available at wileyonlinelibrary.com.]

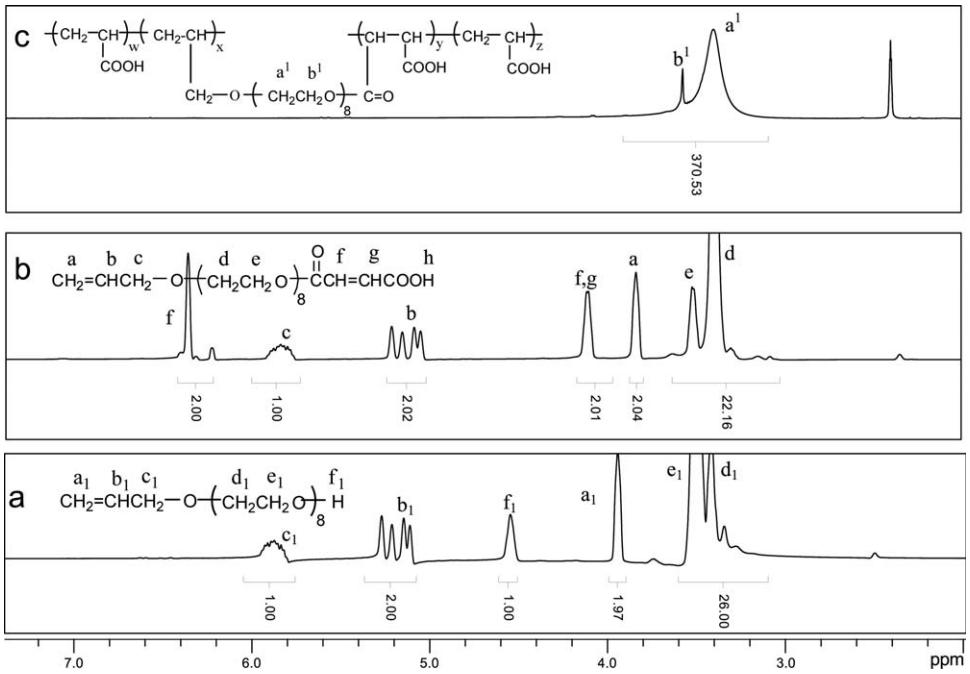

Figure 3. ^{1}H NMR spectra of APEG (a), APEY (b), and AA-APEY (c).

were purified by acetone. After that, the molecular mass distributions of the AYs samples were investigated via GPC and the results are illustrated in Table I. The weight-average molecular weight (M_w) ranged from 1.83×10^4 to 2.17×10^4 as the variation of AA/APEY ratios. However, the polydispersity index (PD) was in range from 1.03 to 1.10, which strongly suggests that the monomers satisfactorily undergo copolymerization to produce uniform copolymers. The GPC response curve of AY_2 showed in Figure 1 also indicates a typical high molecular weight product of copolymerization. Molar mass at the maximum peak (M_p), viscosity-average molecular weight (M_v) and the *z*-average molecular weight (M_z) were also obtained in the curve profiles.

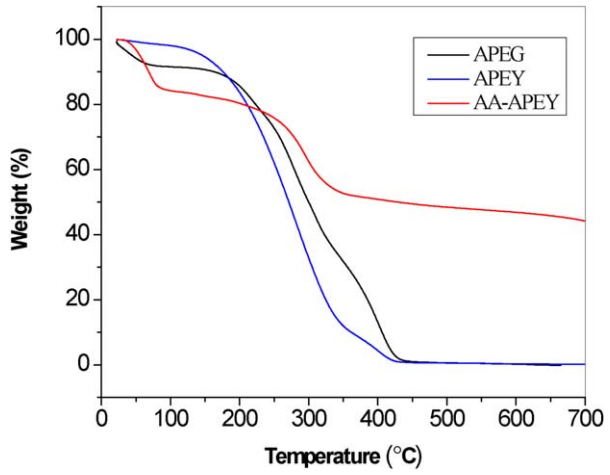

Figure 4. TGA thermograms of APEG, APEY, and AA-APEY under N_2 atmosphere at a heating rate of 10°C min^{-1}. [Color figure can be viewed in the online issue, which is available at wileyonlinelibrary.com.]

FT-IR Analysis of AA-APEY

The FT-IR spectra of APEG, APEY, and AA-APEY (AY_2) are exhibited in Figure 2. Compared with curve a, the emerging 1733 cm^{-1} strong intensity absorption peak (—C═O) in curve *b* indicates that APEY has been synthesized successfully. The fact that the (—C═C—) stretching vibration at 1642 cm^{-1} appears in curve b but disappears completely in curve c reveals that free radical copolymerization between APEY and AA has happened.

^{1}H NMR Analysis of AA-APEY

The structures of the synthesized copolymers were further characterized by the ^{1}H NMR spectra of APEG, APEY, and AA-APEY (AY_2) in Figure 3.

APEG [$(CD_3)_2SO$, δ, ppm]: 2.50 (solvent residual peak of $(CD_3)_2SO$), 3.19–3.61 (—OCH_2CH_2—, ether groups), 3.88–4.01 (CH_2═CH—CH_2—, propenyl protons), 4.51–4.60 (—OH, active hydrogen in APEG), 5.09–5.95 (CH_2═CH—CH_2—, propenyl protons) [Figure 3(a)].

AA-APEY [$(CD_3)_2SO$, δ, ppm]: 2.50 (solvent residual peak of $(CD_3)_2SO$), 3.18–3.65 (—OCH_2CH_2—, ether groups) [Figure 3(c)].

Table II. Thermal Analysis Report of YAs

	First stage		Second stage		Third stage	
Sample	*T* (°C)	*m*[a] (%)	*T* (°C)	*m* (%)	*T* (°C)	*m* (%)
AY_1	42-80	27	229-367	23	400-700	4
AY_2	33-75	17	236-357	32	400-700	6
AY_3	35-81	15	220-334	35	400-700	4
AY_4	40-85	9	235-356	38	400-700	5
AY_5	36-98	7	243-344	43	400-700	2

[a] Weight loss during the temperature rise.

Table III. Calcium Sulfate Inhibition of YAs

Sample	AA/APEY molar ratio	Maximum $CaSO_4$ inhibition (%)	Minimum dosage[a] (mg L^{-1})
AY_1	5 : 1	89.3	5
AY_2	3 : 1	98.4	3
AY_3	1 : 1	94.3	4
AY_4	1 : 3	84.5	7
AY_5	1 : 5	78.9	9

[a] Required minimum dosage to obtain maximum $CaSO_4$ inhibition.

The disappeared peak at 4.51–4.60 ppm in Figure 3(b) reveals that active hydroxyl group of APEG has reacted with maleic anhydride, which confirms the FT-IR analysis of emerging 1733 cm^{-1} strong intensity absorption peak (—C═O) in Figure 2(b). The fact that the double bond absorption peaks (5.05–5.95 ppm) completely disappeared in Figure 3(c) confirms the vanishing (—C═C—) stretching vibration at 1642 cm^{-1} in Figure 2(c). These results prove the successful copolymerization of the monomers.

Thermal Stability Analysis of the AYs

The thermal stability of APEG, APEY, and AA-APEY (AY_2) was investigated using TGA techniques under N_2 atmosphere at a heating rate of 10°C min^{-1} from 30 to 700°C. Figure 4 shows the TGA thermograms of polyether monomer and copolymers. APEG undergoes a small weight loss up to 100°C, while APEY shows no decomposition until 150°C. The polymers have the same repeating units and equal length of ethylene oxide chain, therefore, their differences in thermal stability must be attributed to differences in their end groups. The first stage showed

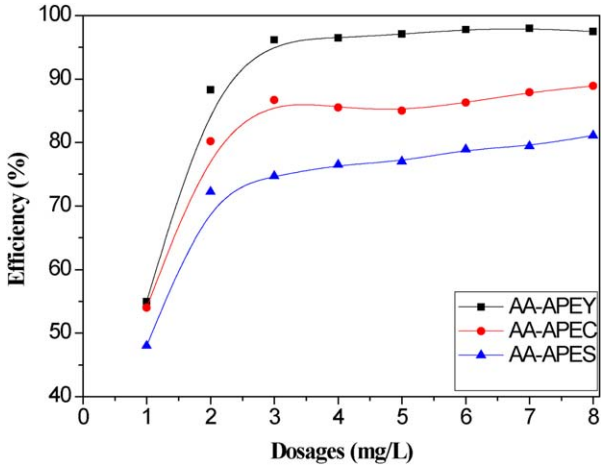

Figure 5. Calcium sulfate inhibition of AA-APEY, AA-APEC, and AA-APES. [Color figure can be viewed in the online issue, which is available at wileyonlinelibrary.com.]

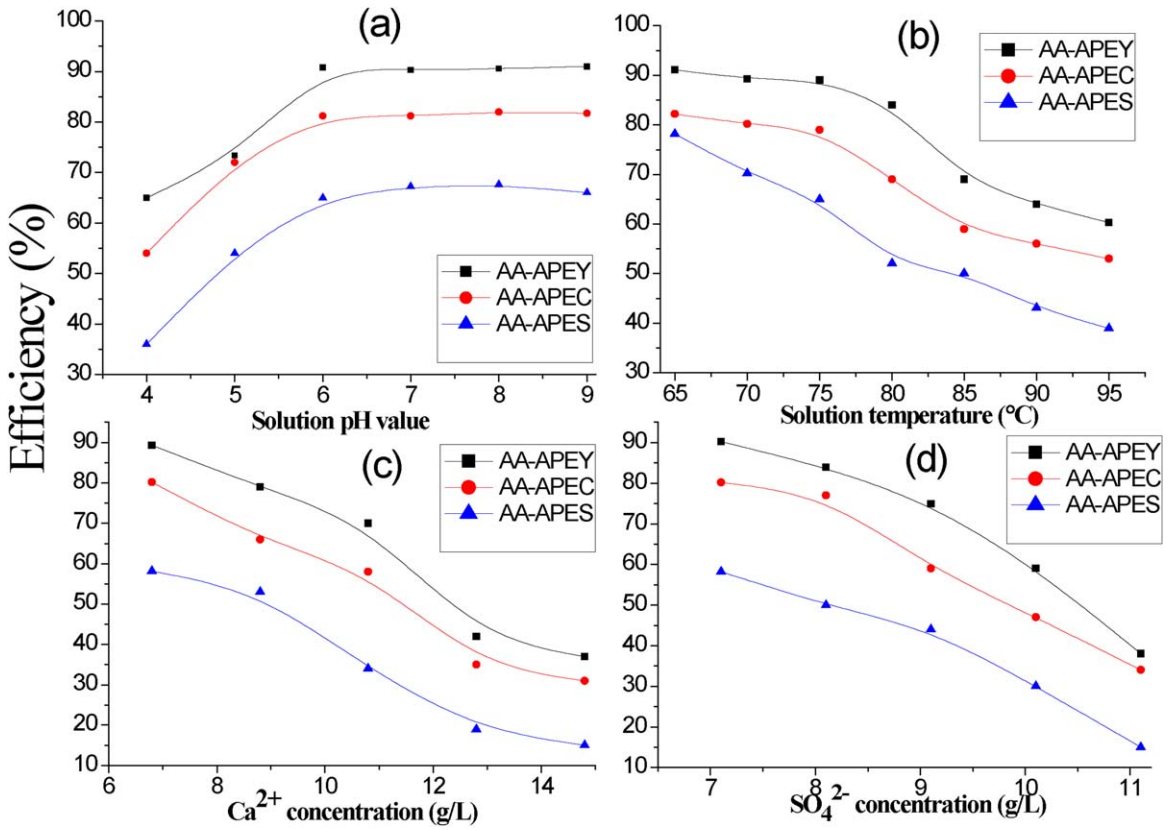

Figure 6. Copolymer inhibition at 2 mg L^{-1} dosage as a function of solution pH (a), temperature (b), Ca^{2+} concentration (c), and SO_4^{2-} concentration (d). [Color figure can be viewed in the online issue, which is available at wileyonlinelibrary.com.]

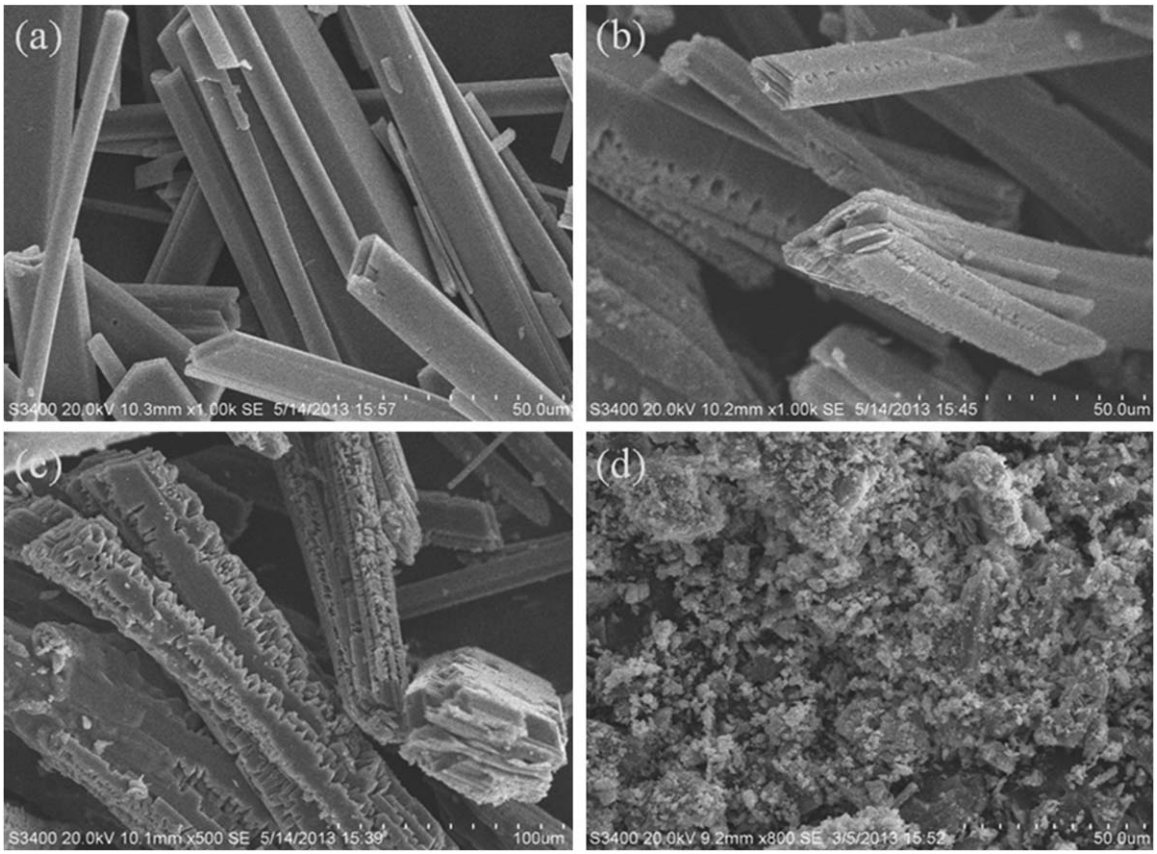

Figure 7. SEM images of calcium sulfate crystals in the absence of AY (a), in the presence of 1 mg L^{-1} AY (b), in the presence of 3 mg L^{-1} AY (c), and in the presence of 5 mg L^{-1} AY (d).

decomposition of active hydroxyl groups (—OH) and evaporation of few water in APEG. After esterizing with maleic anhydride, this region is not observed in curve of APEY, which confirms that the end-capped carboxylic groups (—COOH) in maleic acid are more stable than —OH groups in APEG.[21] Both APEG and APEY were degraded completely at 450°C, while AA-APEY shows just 50% weight loss. It is largely a consequence of the ultrahigh molecular weight copolymers produced by solid-phase copolymerization between the residual carbon-carbon double bond under the condition of high temperature.[23] AA-APEY clearly has the highest thermal stability among the samples.

To further investigate the thermal behavior of AA-APEY (AYs) with different AA-to-APEY mole ratios, their thermogravimetric data were analyzed and the result is presented in Table II. AYs clearly have excellent thermal stability, which is similar to AY_2. There were three degradation stages in the thermograms for these copolymers. The first stage showed a small decomposition of active —OH groups and residual water at 30–100°C. The second stage mass loss was observed at the temperature range of 22–370°C, with a total of 23–43% mass loss. Only about 5% weight loss was obtained up to 700°C in the third stage, further supporting the previously discussed analysis of the form of ultrahigh molecular weight copolymers.

Inhibition Behaviors

The ability of AYs to control $CaSO_4$ deposits was prepared at different AA/APEY mole ratio as shown in Table III. According to the dates, the maximum inhibition rate of AY_1, AY_3, AY_4, and AY_5 were respectively, 89, 94, 89, and 79%, which were absolutely below 98% for AY_2. It is obvious that AY_2 shows the best anti-scaling performance which obtains maximum $CaSO_4$ inhibition (%) at a level of 3 mg L^{-1}.

The performance of AA-APEY (AY_2) on $CaSO_4$ inhibition was then compared with other tow polyether-based polycarboxylates (AA-APEC and AA-APES), which are similar to AA-APEY in

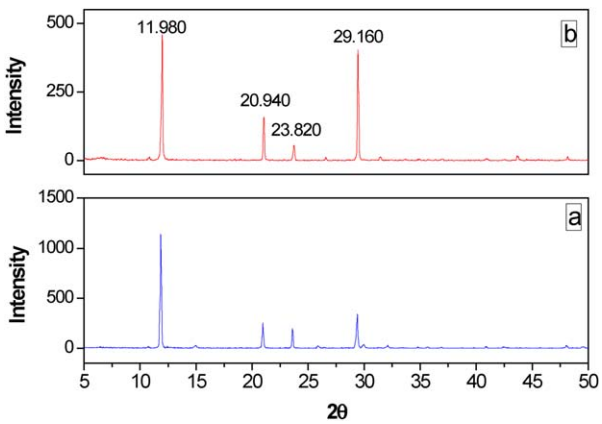

Figure 8. The XRD pattern of the $CaSO_4$ crystals in the absence of AY (a), and in the presence of 5 mg L^{-1} AY (b). [Color figure can be viewed in the online issue, which is available at wileyonlinelibrary.com.]

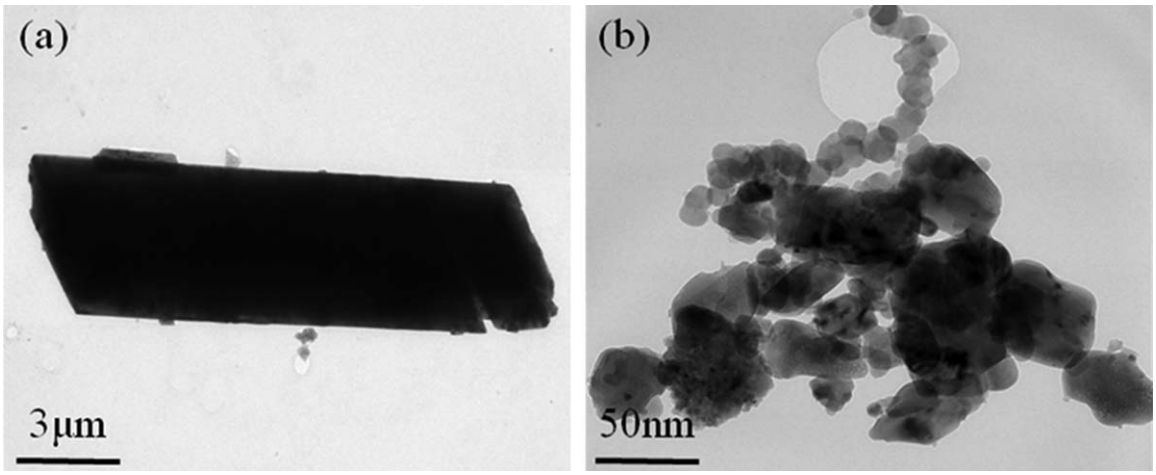

Figure 9. The TEM micrographs of $CaSO_4$ in the absence of AY (a), and in the presence of 5 mg L^{-1} AY (b).

structure (Figure 5). It is clear that all of the three inhibitors exhibits an obvious "threshold effect," namely, the inhibition efficiency does not obviously increase correspondingly when the concentration of inhibitor exceeds a certain limit. AA-APEY displays superior ability to control $CaSO_4$ deposition with 96% inhibition at threshold dosage of 3 mg L^{-1}, whereas it is 85% for AA-APEC at the same dosage. AA-APES showed the poorest inhibition with 70% inhibition at threshold dosage of 4 mg L^{-1}. The phenomenon that AA-APEY displayed the best inhibition efficiency can be attributed to that AA-APEY copolymers contain more acidic carboxylic acid (—COOH) groups.[24]

The effect of different solution properties on the $CaSO_4$ inhibition of AA-APEY (AY_2), AA-APEC and AA-APES were investigated and the result is presented in Figure 6. Variable-controlling method was used under the standard solution parameters of $[Ca^{2+}] = 6.8$ (6.8 g L^{-1} Ca^{2+}), $[SO_4^{2-}] = 7.1$ (7.1 g L^{-1} SO_4^{2-}), pH = 7.0, $T = 70°C$, $t = 6.0$ h.

As exhibited in Figure 6(a), at a pH of 4.0–6.0, the efficiency of all the three inhibitors increased with the increasing of pH while the inhibition was tending towards stability at a pH of 6.0–9.0. The scale inhibition is 20% lower at lower pH probably due to the protonation of active functionality of antiscalant, i.e., —COOH groups. Moreover, AA-APEY showed superior inhibition than AA-APEC and AA-APES in a wider range of pHs. At pH = 7.0, under the same standard parameters, the influence of the temperature was shown in Figure 6(b). It is clear that polyether-based inhibitors have a good thermal stability when solution temperature is below 80°C. Figure 6(c,d) demonstrates the effect of high concentration of Ca^{2+} and SO_4^{2-}, respectively. The inhibitory power of investigated inhibitors decrease with the increasing of both $[Ca^{2+}]$ and $[SO_4^{2-}]$. What's more, compared to $[SO_4^{2-}]$, the influence of $[Ca^{2+}]$ is much more serious on the efficiency.

According to the parallel tests above, compared with AA-APEC and AA-APES, AA-APEY has the best scale inhibition on calcium sulfate deposits at a lower dosage under the standard solution conditions. In addition, it can be used under a harsher water quality: pH = 6–9, $T = 70$–$80°C$, $[Ca^{2+}] = 6.8$–8.8 g L^{-1}, $[SO_4^{2-}] = 7.1$–9.1 g L^{-1}.

Morphology Studies of $CaSO_4$ Precipitation

Calcium sulfate crystals were examined by SEM to characterize morphological changes that happened during growth without and with addition of AY (Figure 7). It is clear that, uninhibited seeds consisted of thin needle-shaped crystals with an elongated monoclinic structure [Figure 7(a)], which are similar to the earlier reports.[6,25] In the presence of 1 mg L^{-1} AY, small cracks occurred in the surface of crystals. In the presence of 3 mg L^{-1} AY, massive cracks and fractured layer structure were obtained, while adding up to 6 mg L^{-1} AY, the crystals were completely changed to irregular particles [Figure 7(b–d)]. In addition, the more dosage is, the stronger the influence is on calcium sulfate crystal morphology. It indicates that the inhibitor of AY copolymers obviously decrease the size of $CaSO_4$ deposition particles thereby dispersing them in a fluid.

To identify the crystal form of $CaSO_4$ in the absence and presence of AY, XRD measurements were carried out and the result is shown in Figure 8. It can be inferred that the structure is proved to be $CaSO_4 \cdot 2H_2O$ according to the 2θ values from both Figure 8(a,b).[26] XRD results show that crystal structure has been just weakened not altered, which can be confirmed by the variation in the intensity values and no change in 2θ values.

The inferences about morphology changes mentioned above were further proofed through TEM micrograph. As showed in

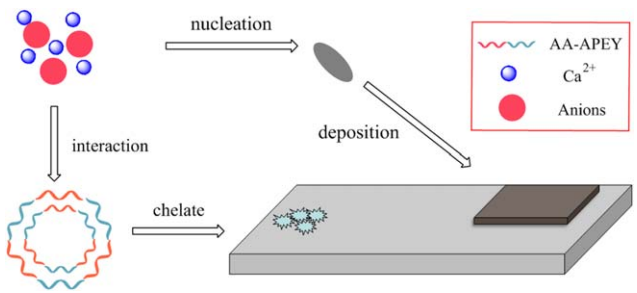

Figure 10. Schematic illustration of scale deposition in the absence and presence of AY. [Color figure can be viewed in the online issue, which is available at wileyonlinelibrary.com.]

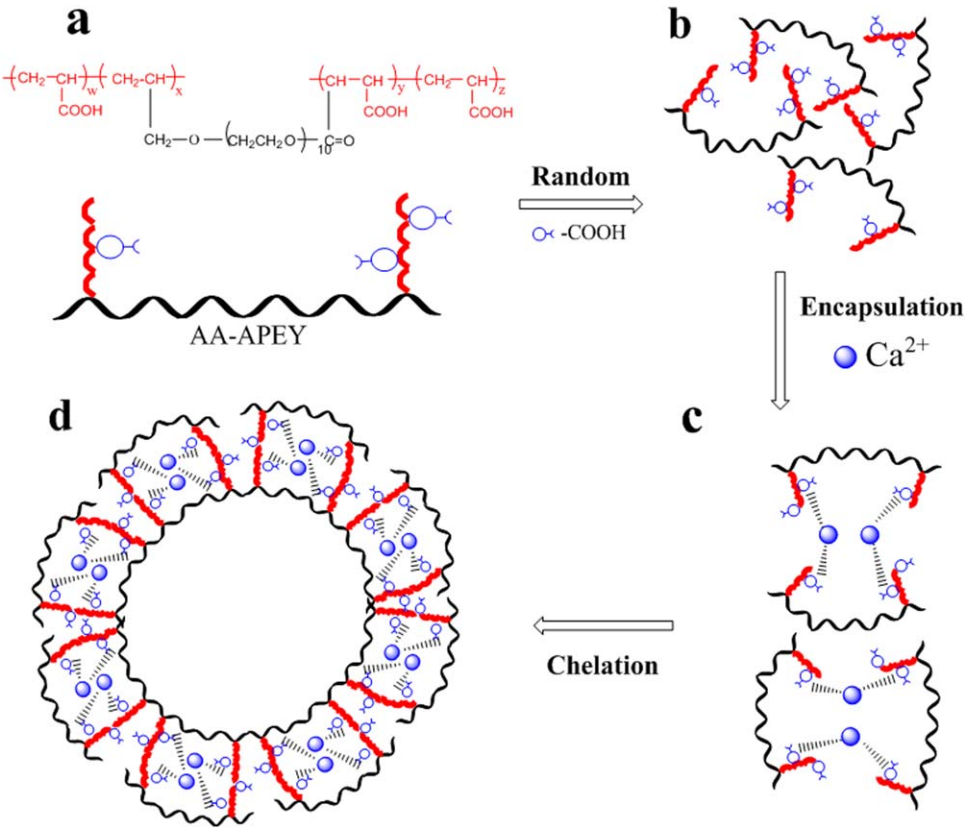

Figure 11. Schematic illustration of chelation mechanism. [Color figure can be viewed in the online issue, which is available at wileyonlinelibrary.com.]

Figure 9, the monoclinic crystal structure with an edge length of around 10 μm was obtained in the absence of AY, while in the presence of 5 mg L^{-1} AY, the size of $CaSO_4$ crystals decreased to 50–200 nm. However, diamond-shaped crystals were still existed among the interpenetrated conglomerates, which is coincident exactly with the results of XRD.

Chelation Mechanism of Calcium Sulfate Inhibition

There are many theories about the mechanism of calcium sulfate inhibition, such as chelating solubilization, a multilayer type of adsorption on the scale surface, and electrostatic repulsion function. However, chelation mechanism has gained extensive acceptance currently.[2] According to this theory, massive —COOH groups in AA-APEY retard scale formation by interfering crystal formation through chelation.[27,28] In the absence of AY, $CaSO_4$ crystals grow regularly with an unbroken smooth surface in pipes, which seems to fit the micro-morphology of $CaSO_4$ crystals in Figures 7(a) and 9(a). After interacting with AY, nucleation and crystal growth of $CaSO_4$ are irregular, which can be confirmed by Figures 7(d) and 9(b). The schematic illustration of scale deposition in the absence and presence of AY was shown in Figure 10.

AA and APEY blocks, which are hydrophilic chain segments, originally distribute in water at first [Figure 11(b)]. Once confronted with Ca^{2+} ions, the —COOH groups of AA-APEY can recognize and react with the positively charged ions, which would leads to the spontaneous formation of AA-APEY-Ca complexes [Figure 11(c)]. In this case, Ca^{2+} acting as ties simultaneously link AA-APEY through carboxyl groups and SO_4^{2-} ions through electrostatic attractive force. Thereafter, a three-decker structure of PEG (outer shell), —COOH-Ca complexes (middle layer) and PEG (inner shell) is formed [Figure 11(d)]. And these chelate compounds are stable toward aqueous phase because of the encapsulated hydrophilic polyethylene glycol (PEG) segments.[15,29–32] In this case, the inhibition efficiency is more pronounced with more carboxylate-containing groups. The mechanism procedure of chelation is showed in Figure 11.

CONCLUSIONS

A phosphorous free, nonsulfur and nonnitrogen inhibitor, the copolymer of AA-APEY was synthesized with different AA/APEY ratios in this study. The synthesized copolymers were characterized by FT-IR and further conformed by ^{1}H-NMR. The molecular mass distribution of AYs indicates that monomers satisfactorily undergo copolymerization to produce uniform copolymers. AY_2 shows the best thermal stability among the series of AYs. AA-APEY is more efficient than other tow polyether-based polycarboxylate antiscalants, showing ~96% inhibition at threshold dosage of 3 mg L^{-1} whereas AA-APEC and AA-APES exhibited only 65–80% inhibition. SEM, XRD and TEM analyses indicate that morphology of calcium sulfate is completely changed and the crystal structure has been weakened in the presence of AA-APEY. The inhibition mechanism toward calcium sulfate deposits was supposed to be the

formation of soluble AA-APEY-Ca complexes instead of forming $CaSO_4$ crystal embryos directly.

ACKNOWLEDGMENTS

This work was supported by the Prospective Joint Research Project of Jiangsu Province (BY2012196); The National Natural Science Foundation of China (51177013); Special funds for Jiangsu Province Scientific and Technological Achievements Projects of China (BA2011186); Program for Training of 333 High-Level Talent, Jiangsu Province of China (BRA2011033); Scientific Innovation Research Foundation of College Graduate in Jiangsu Province (CXLX13-107).

REFERENCES

1. Wang, C.; Zhu, D. Y.; Wang, X. K. *J. Appl. Polym. Sci.* **2011**, *115*, 2149.
2. Hasson, D.; Shemer, H.; Sher, A. *Ind. Eng. Chem. Res.* **2011**, *50*, 7601.
3. Rahardianto, A.; Shih, W. Y.; Lee, R. W.; Cohen, Y. *J. Membr. Sci.* **2006**, *279*, 655.
4. Sarig, S.; Mullin, J. W. *J. Chem. Technol. Biotechnol.* **1982**, *32*, 525.
5. Tang, Y. M.; Yang, W. Z.; Yin, X. S. *Desalination* **2008**, *228*, 55.
6. Amjad, Z. *Desal. Wat. Treat.* **2011**, *36*, 270.
7. Bahadur, A. *Mater. Trans.* **1996**, *37*, 605.
8. Moudgil, H. K.; Yadav, S.; Chaudhary, R. S.; Dheeraj, K. *J. Appl. Electrochem.* **2009**, *39*, 1339.
9. Tomson, M. B.; Kan, A. T.; Oddo, J. E. *Langmuir.* **1994**, *11*, 1442.
10. Dyer, S. J.; Anderson, C. E.; Graham, G. M. *J. Petrol. Sci. Eng.* **2004**, *43*, 259.
11. Xyla, A. G.; Mikroyannidis, J.; Koutsoukos, P. G. *J. Colloid Interface Sci.* **1992**, *153*, 537.
12. Rieger, J.; Thieme, J.; Schmidt, C. *Langmuir* **2000**, *16*, 8300.
13. Reddy, M. M.; Hoch, A. R. *J. Colloid Interface Sci.* **2001**, *235*, 365.
14. Dietzsch, M.; Barz, M.; Schuler, T. *Langmuir* **2013**, *29*, 3080.
15. Tsortos, A.; Nancollas, G. H. *J. Colloid Interface Sci.* **2002**, *250*, 159.
16. Butt, F. H.; Rahman, F.; Baduruthamal, U. *Desalination* **1995**, *111*, 219.
17. Gill, J. S. *Desalination* **1999**, *124*, 43.
18. Benbakhti, A.; Bachir-Bey, T. *J. Appl. Polym. Sci.* **2011**, *116*, 3095.
19. Nederlof, M. M.; Paassen, J. V.; Jong, R. *Desalination* **2005**, *178*, 303.
20. Du, K.; Zhou, Y. M.; Wang, Y. Y. *J. Appl. Polym. Sci.* **2009**, *113*, 1966.
21. Steckler, R. US Patent 3,875,202, **1975**.
22. Sevim, U. C.; Ayhan, B. *Curr. Appl. Phys.* **2013**, *13*, 1668.
23. Fu, C. E.; Zhou, Y. M.; Xie, H. T.; Sun, W.; Wu, W. D. *Ind. Eng. Chem. Res.* **2011**, *49*, 8920.
24. Lee, S.; Lee, C. H. *Water Res.* **2000**, *34*, 3854.
25. Ling, Y. B.; Demopoulos, G. P. *Ind. Eng. Chem. Res.* **2005**, *44*, 715.
26. Hasson, D.; Zahavi, J. *Ind. Eng. Chem. Res.* **1970**, *9*, 1.
27. Yu, S. H.; Colfen, H.; Antonietti, M. *J. Phys. Chem.* **2003**, *117*, 379.
28. Rudloff, J.; Colfen, H. *Langmuir* **2004**, *20*, 991.
29. Harada, A.; Kataoka, K. *Langmuir* **1999**, *15*, 4208.
30. Scholz, C.; Iijima, M.; Nagasaki, Y.; Kataoka, K. *Macromolecules* **1995**, *28*, 7295.
31. Abd-El-Khalek, D. E.; Abd-El-Nabey, B. A. *Desalination* **2013**, *311*, 227.